

Conformational properties of complex polymers: rosette versus star-like structures

This content has been downloaded from IOPscience. Please scroll down to see the full text.

2015 J. Phys. A: Math. Theor. 48 135001

(<http://iopscience.iop.org/1751-8121/48/13/135001>)

View [the table of contents for this issue](#), or go to the [journal homepage](#) for more

Download details:

This content was downloaded by: metzler

IP Address: 141.89.176.192

This content was downloaded on 16/04/2015 at 09:37

Please note that [terms and conditions apply](#).

Conformational properties of complex polymers: rosette versus star-like structures

V Blavatska¹ and R Metzler^{2,3}

¹Institute for Condensed Matter Physics of the National Academy of Sciences of Ukraine, 79011 Lviv, Ukraine

²Institute for Physics and Astronomy, University of Potsdam, D-14476 Potsdam-Golm, Germany

³Department of Physics, Tampere University of Technology, FI-33101 Tampere, Finland

E-mail: viktorija@icmp.lviv.ua

Received 25 November 2014, revised 19 January 2015

Accepted for publication 10 February 2015

Published 10 March 2015



CrossMark

Abstract

Multiple loop formation in polymer macromolecules is an important feature of the chromatin organization and DNA compactification in the nuclei. We analyse the size and shape characteristics of complex polymer structures, containing in general f_1 loops (petals) and f_2 linear chains (branches). Within the frames of continuous model of Gaussian macromolecule, we apply the path integration method and obtain the estimates for gyration radius R_g and asphericity \hat{A} of typical conformation as functions of parameters f_1, f_2 . In particular, our results qualitatively reveal the extent of anisotropy of star-like topologies as compared to the rosette structures of the same total molecular weight.

Keywords: polymers, path integration, conformational properties

(Some figures may appear in colour only in the online journal)

1. Introduction

Loop formation in macromolecules plays an important role in a number of biochemical processes: stabilization of globular proteins [1–4], transcriptional regularization of genes [5–7] as well as DNA compactification in the nucleus [8–10]. The localization of chromatin fibres to semi-compact regions known as chromosome territories is maintained among others by the topological constraints introduced by multiple loops in chromatin organization [11].

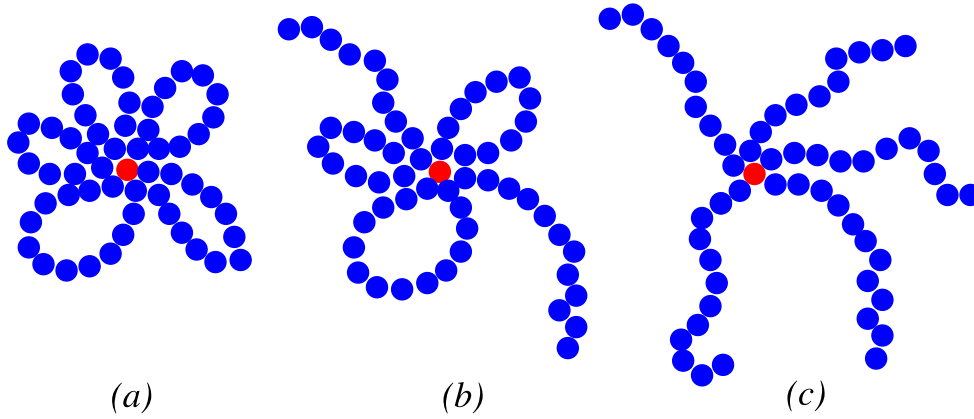


Figure 1. Schematic presentation of polymer systems of complex topologies.

Numerous analytical and numerical studies have been conducted to analyse the cyclization probability and loop size distributions in long flexible macromolecules [12–19]. The conformational properties of isolated loops (ring polymers) [20–32] and multiple loops [10, 33] have been intensively studied as well.

Interlocking and entanglements are ubiquitous features of flexible polymers of high molecular weight. In particular, DNA can exist in the form of catenated (bonded) rings of various complexities [34–36]. The segments of different DNA molecules can intercross through the transient breaks introduced by special enzymes (topoisomerases) [37–39]. Numerous studies [40–47] reveal the advantage of linking in stabilization of peptide and protein oligomers.

In this respect, it is worthwhile studying the conformational properties of generalized complex polymer structures containing f_1 loops and f_2 linear chains of the same length S (see figure 1). The properties of so-called ‘rosette’ (figure 1(a)) and ‘ring-linear’ (figure 1(b)) structures have been considered recently in numerical simulations in [11, 48]. However, only the shape properties of very simple structures of two bonded rings ($f_2 = 2, f_1 = 0$) and rings with two connected linear branches ($f_2 = 1, f_1 = 2$) with excluded volume effects were analysed [48]. In particular, a subtle difference in the conformational properties of two connected polymer rings compared with that of one isolated ring were found. On the other hand, the properties of ‘star’ polymers (figure 1(c)) have been intensively studied [49–57].

In general, the statistics of polymers is known to be characterized by a set of universal properties, which are independent of the details of the microscopic chemical structure [58, 59]. In particular, the asymptotic number of possible conformations of the structure shown in figure 1(b) obeys the scaling law [49]

$$\mathcal{Z}_{f_1 f_2} \sim \mu^{(f_1 + f_2)S} S^{\gamma_{f_1 f_2} - 1}, \quad \gamma_{f_1 f_2} = 1 - \nu f_1 + \sigma_{2f_1 + f_2} + f_2 \sigma_1. \quad (1)$$

Here, ν is the universal critical (Flory) exponent, governing the scaling of the size measure (e.g. the averaged gyration radius R_g) of macromolecule according to

$$\langle R_{g, f_1 f_2}^2 \rangle \sim ((f_1 + f_2)S)^{2\nu}, \quad (2)$$

σ_i is the set of so-called vertex exponents (with $\sigma_2 = 0$), d is the spatial dimension and μ is a non-universal fugacity. For an idealized Gaussian (phantom) macromolecule without any interactions between monomers, one finds $\nu = 1/2$, $\sigma_i = 0$. In the limiting cases ($f_1 = 0$) and ($f_2 = 0$), we obtain the corresponding critical exponents, governing the scaling of the number of possible conformations of f_2 -branch star and f_1 -petal rosette polymers: $\gamma_{\text{star}} = 1$, $\gamma_{\text{rosette}} = 1 - df_1/2$. Therefore, additional topological constraints in rosette polymers lead to a considerable reduction of the number of allowed conformations, as compared with star polymers of the same molecular weight.

To compare the size measures of macromolecules of different topologies but of the same total molecular weight, one can consider the universal size ratios. In particular, in the idealized Gaussian case, the ratio of the gyration radii of the individual ring and open linear structures reads [60]

$$\frac{\langle R_{\text{g ring}}^2 \rangle}{\langle R_{\text{g linear}}^2 \rangle} = \frac{1}{2}, \quad (3)$$

whereas comparing the size of f -branch star and a linear chain of the same total length one has [60]

$$\frac{\langle R_{\text{g fstar}}^2 \rangle}{\langle R_{\text{g linear}}^2 \rangle} = \frac{3f - 2}{f^2}. \quad (4)$$

Taking into account the excluded volume effect leads to an increase of this values [51, 61–66].

The overall shape of a typical polymer conformation is of great importance affecting, in particular, the mobility and folding dynamics of proteins [67, 68]. The shape of DNA may be relevant for the accessibility for enzymes depending on the spatial distance between DNA-segments [69]. Already in 1934 it was realized [70] that the shape of a typical flexible polymer coil in a solvent is anisotropic and resembles that of a prolate ellipsoid. It is convenient to characterize the asymmetry of polymer configurations in terms of rotationally invariant universal quantities [71, 72] constructed as combinations of the components of the gyration tensor, such as the asphericity \hat{A} . This quantity takes on a maximum value of unity for a completely stretched, rod-like configuration, and equals zero for the spherical form thus obeying the inequality $0 \leq \hat{A} \leq 1$. In the Gaussian case, for the individual linear and circular polymer chains one has correspondingly [72]

$$\hat{A}_{\text{linear}} = \frac{2(d+2)}{5d+4}, \quad (5)$$

$$\hat{A}_{\text{ring}} = \frac{d+2}{5d+2}, \quad (6)$$

whereas the asphericity of f -branch star polymer reads [73]:

$$\hat{A}_{\text{star}} = 2 \frac{(2+d)(15f-14)}{5d(3f-2)^2 + 4(15f-14)}. \quad (7)$$

Note that equation (5) gives the asphericity of a trajectory of a diffusive randomly walking particle. The influence of excluded volume effects on the shape parameters of single linear and ring polymers, as well as star polymers, have been analysed so far both analytically [22, 71, 74] and numerically [75–79].

In this paper, we study the universal size and shape characteristics of complex polymer structures (figure 1), applying the path integration method. Special attention is paid to the analytical study of statistical properties of rosette (figure 1(a)) and ring-linear (figure 1(b)) structures.

The layout of the paper is as follows. In section 2, we briefly describe the presentation of complex polymer system within the frames of continuous chain model. Our results are given in section 3. We finish by giving conclusions in section 4.

2. The model

We consider a system consisting of f_1 closed polymer loops (petals) and f_2 linear chains (branches) all bonded together at one ‘branching’ point (see figure 1(b)). Within the Edwards’ continuous chain model [80], each of the individual branches or petals is presented as a path of length S_i , parameterized by $\vec{r}_i(s)$, where s is varying from 0 to S_i ($i = 1, 2, \dots, f_1 + f_2$). For simplicity we take $S_1 = \dots = S_{f_1+f_2} = S$. The weight of the individual i th path is given by

$$W_i = \exp\left(-\frac{1}{2} \int_0^S \left(\frac{d\vec{r}_i(s)}{ds}\right)^2 ds\right) \quad (8)$$

and the partition function of the system can thus be written as

$$\mathcal{Z}_{f_1, f_2} = \frac{\int \mathcal{D}\vec{r} \prod_{j=1}^{f_1} \delta(\vec{r}_j(S) - \vec{r}_j(0)) \prod_{i=1}^{f_1+f_2} \delta(\vec{r}_i(0)) W_i}{\int \mathcal{D}\vec{r} \prod_{i=1}^{f_1+f_2} \delta(\vec{r}_i(0)) W_i}. \quad (9)$$

Here, $\int \mathcal{D}\vec{r}$ denotes functional path integrations over $f_1 + f_2$ trajectories. The products of δ -functions describe the fact that f_1 trajectories are closed and that the starting point of all trajectories is fixed (the branching point). Note, that (9) is normalized in such a way that the partition function of the system consisting of $f_1 + f_2$ open linear Gaussian chains (star-like structure) is unity.

Exploiting the Fourier transform of the δ -functions

$$\delta(\vec{r}_j(S) - \vec{r}_j(0)) = (2\pi)^{-d} \int d\vec{q}_j e^{-i\vec{q}_j(\vec{r}_j(S) - \vec{r}_j(0))} \quad (10)$$

and rewriting in the exponent

$$-\frac{1}{2} \int_0^S \left(\frac{d\vec{r}_j(s)}{ds}\right)^2 ds - i\vec{q}_j \int_0^S \frac{d\vec{r}_j(s)}{ds} ds = -\frac{1}{2} \int_0^S ds \left(\left(\frac{d\vec{r}_j(s)}{ds} + i\vec{q}_j\right)^2 + q^2 \right)$$

we evaluate the expression of partition function (9), giving the asymptotic number of possible conformations of polymer system

$$\mathcal{Z}_{f_1, f_2} = (2\pi)^{-f_1 d} \prod_{j=1}^{f_1} \int d\vec{q}_j e^{-\frac{q_j^2 S}{2}} = (2\pi S)^{-df_1/2}. \quad (11)$$

Comparing this relation with equation (1), we recover the estimate for the critical exponent $\gamma_{f_1, f_2} = 1 - df_1/2$.

The average of any observable $\langle(\dots)\rangle$ over an ensemble of conformations is then given by

$$\langle(\dots)\rangle = \frac{1}{Z_{f_1 f_2}} \frac{\int \mathcal{D}\vec{r} \prod_{j=1}^{f_1} \delta(\vec{r}_j(S) - \vec{r}_j(0)) \prod_{i=1}^{f_1+f_2} \delta(\vec{r}_i(0))(\dots) W_i}{\int \mathcal{D}\vec{r} \prod_{i=1}^{f_1+f_2} \delta(\vec{r}_i(0)) W_i}. \quad (12)$$

3. Size ratios and asphericity

The size and shape characteristics of a typical polymer conformation can be characterized [79] in terms of the gyration tensor \mathbf{Q} . Within the framework of a continuous polymer model the components of this tensor can be presented as

$$Q_{\alpha\beta} = \frac{1}{2S^2(f_1 + f_2)^2} \sum_{i,j=1}^{f_1+f_2} \int_0^S ds_1 \int_0^S ds_2 (\vec{r}_i^\alpha(s_2) - \vec{r}_j^\alpha(s_1)) (\vec{r}_i^\beta(s_2) - \vec{r}_j^\beta(s_1)), \quad (13)$$

where $r_i^\alpha(s_1)$ is α th component of $\vec{r}_i(s_1)$ ($\alpha = 1, 2, \dots, d$).

For the averaged radius of gyration one has

$$\begin{aligned} \langle R_{g,f_1 f_2}^2 \rangle &= \frac{1}{2S^2(f_1 + f_2)^2} \sum_{i,j=1}^{f_1+f_2} \left\langle \int_0^S ds_1 \int_0^{s_1} ds_2 (\vec{r}_i(s_2) - \vec{r}_j(s_1))^2 \right\rangle \\ &= \langle \text{Tr } \mathbf{Q} \rangle. \end{aligned} \quad (14)$$

Here and below, $\langle(\dots)\rangle$ denotes averaging over an ensemble of path conformations according to (12).

The spread in the eigenvalues λ_i of the gyration tensor (13) describes the distribution of monomers inside the polymer coil and thus measures the asymmetry of the molecule. For a symmetric (spherical) configuration all the eigenvalues λ_i are equal, whereas for a completely stretched rod-like conformation all λ_i are zero except one. Let $\bar{\lambda} \equiv \text{Tr } \mathbf{Q}/d$ be the mean eigenvalue of the gyration tensor. Then one may characterize the extent of asphericity of a macromolecule by the quantity \hat{A} defined as [71]:

$$\hat{A} = \frac{1}{d(d-1)} \sum_{i=1}^d \frac{\langle (\lambda_i - \bar{\lambda})^2 \rangle}{\langle \bar{\lambda}^2 \rangle} = \frac{d}{d-1} \frac{\langle \text{Tr } \hat{\mathbf{Q}}^2 \rangle}{\langle (\text{Tr } \mathbf{Q})^2 \rangle}, \quad (15)$$

with $\hat{\mathbf{Q}} \equiv \mathbf{Q} - \bar{\lambda} \mathbf{I}$ (here \mathbf{I} is the unity matrix). This universal quantity equals zero when $\lambda_i = \bar{\lambda}$ and takes a maximum value of one in the case of a rod-like configuration. The asphericity (15) can be rewritten in terms of the averaged components of the gyration tensor (13) as follows [71]:

$$\hat{A} = \frac{\langle Q_{\alpha\alpha} Q_{\alpha\alpha} \rangle + d \langle Q_{\alpha\beta} Q_{\alpha\beta} \rangle - \langle Q_{\alpha\alpha} Q_{\beta\beta} \rangle}{\langle Q_{\alpha\alpha}^2 \rangle + (d-1) \langle Q_{\alpha\alpha} Q_{\beta\beta} \rangle}. \quad (16)$$

Below, we give detailed evaluation of the expressions for the averaged radius of gyration (14) and asphericity (16) of the model (9) within the framework of path integration approach.

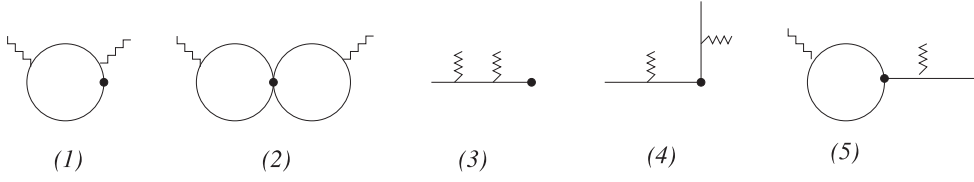


Figure 2. Diagrammatic presentation of contributions into $\langle \xi(\vec{k}) \rangle$. The solid line on a diagram is a schematic presentation of a polymer path of length S , and wavy lines denote so-called restriction points s_1 and s_2 . With \bullet we denote the position of the starting branching point.

3.1. Radius of gyration

The radius of gyration (14) can be calculated from the identity

$$\left(\vec{r}_i(s_2) - \vec{r}_j(s_1) \right)^2 = -2d \frac{\partial}{\partial |k|^2} \xi(\vec{k}) \Big|_{k=0}, \quad \xi(\vec{k}) \equiv e^{i\vec{k} \cdot (\vec{r}(s_2) - \vec{r}(s_1))}, \quad (17)$$

and evaluating $\langle \xi(\vec{k}) \rangle$ in the path integration approach. In calculation of the contributions into $\langle \xi(\vec{k}) \rangle$ it is convenient to use the diagrammatic presentation as given in figure 2. According to the general rules of diagram calculations [59], each segment between any two restriction points s_a and s_b is oriented and bears a wave vector \vec{q}_{ab} given by a sum of incoming and outgoing wave vectors injected at restriction points and end points. At these points, the flow of wave vectors is conserved. A factor, $\exp(-\vec{q}_{ab}^2(s_b - s_a)/2)$, is associated with each segment. An integration is made over all independent segment areas and over wave vectors injected at the end points.

The analytic expressions, corresponding to the diagrams (1)–(5) in figure 2 then read

$$\begin{aligned} \langle \xi(\vec{k}) \rangle_{(1)} &= \left(\frac{S}{2\pi} \right)^{\frac{d}{2}} e^{-\frac{k^2}{2}(s_2-s_1)} \int dq_1 e^{-\frac{q_1^2}{2}S} e^{-kq_1(s_2-s_1)} \\ &= e^{-\frac{k^2}{2} \frac{(s_2-s_1)(S-s_2+s_1)}{S}}, \end{aligned} \quad (18)$$

$$\begin{aligned} \langle \xi(\vec{k}) \rangle_{(2)} &= \left(\frac{S}{2\pi} \right)^d e^{-\frac{k^2}{2}(s_2+s_1)} \int dq_1 \int dq_2 e^{-\frac{q_1^2}{2}S} e^{-\frac{q_2^2}{2}S} e^{-q_1 k s_1} e^{-q_2 k s_2} \\ &= e^{-\frac{k^2}{2} \frac{S(s_1+s_2)-s_1^2-s_2^2}{S}}, \end{aligned} \quad (19)$$

$$\langle \xi(\vec{k}) \rangle_{(3)} = e^{-\frac{k^2}{2}(s_2-s_1)}, \quad (20)$$

$$\langle \xi(\vec{k}) \rangle_{(4)} = e^{-\frac{k^2}{2}(s_2+s_1)}, \quad (21)$$

$$\langle \xi(\vec{k}) \rangle_{(5)} = \left(\frac{S}{2\pi} \right)^{\frac{d}{2}} e^{-\frac{k^2}{2}(s_2+s_1)} \int dq_1 e^{-\frac{q_1^2}{2}S} e^{-kq_1 s_1} = e^{-\frac{k^2}{2} \frac{S(s_1+s_2)-s_1^2}{S}}. \quad (22)$$

Taking the derivatives with respect to k according to (17) in the expressions above and taking into account the combinatorial factors, we find for the radius of gyration

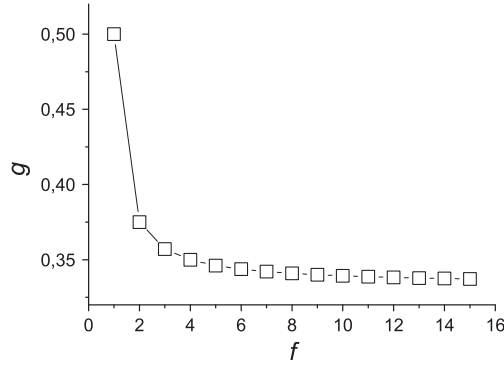


Figure 3. Size ratio (26) of rosette and star polymers of the same total molecular weight as function of branching parameter f . The line is a guide for the eyes.

$$\begin{aligned}
\langle R_{g,f_1,f_2}^2 \rangle &= \frac{Sd}{(f_1 + f_2)^2 S^2} \left(f_1 \int_0^S ds_2 \int_0^{s_2} ds_1 \frac{(s_2 - s_1)(S - s_2 + s_1)}{S} \right. \\
&\quad + \frac{f_1(f_1 - 1)}{2} \int_0^S ds_2 \int_0^S ds_1 \frac{(s_2 - s_1)(S(s_1 + s_2) - s_1^2 - s_2^2)}{S} \\
&\quad + f_2 \int_0^S ds_2 \int_0^{s_2} ds_1 (s_2 - s_1) + \frac{f_2(f_2 - 1)}{2} \int_0^S ds_2 \int_0^S ds_1 (s_2 + s_1) \\
&\quad \left. + f_1 f_2 \int_0^S ds_2 \int_0^S \frac{(s_2 - s_1)(S(s_1 + s_2) - s_1^2)}{S} \right) \\
&= \frac{Sd}{(f_1 + f_2)^2} \frac{1}{12} [f_1(2f_1 - 1) + 2f_2(3f_2 - 2) + 8f_1 f_2]. \tag{23}
\end{aligned}$$

The case $f_2 = 0$ corresponds to the rosette structure (figure 1(a)) with

$$\langle R_{g, \text{rosette}}^2 \rangle = \frac{Sd}{12f_1} (2f_1 - 1), \tag{24}$$

at $f_1 = 1$, one recovers the gyration radius of individual ring polymer. The case $f_1 = 0$ corresponds to star structure (figure 1(c)) with

$$\langle R_{g, \text{star}}^2 \rangle = \frac{Sd}{6f_2} (3f_2 - 2), \tag{25}$$

at $f_2 = 1$, one receives the gyration radius of linear polymer chain.

For the size ratio of rosette and star polymers of the same total molecular weight (corresponding to $f_1 = f_2 = f$) we obtain

$$g \equiv \frac{\langle R_{g, \text{rosette}}^2 \rangle}{\langle R_{g, \text{star}}^2 \rangle} = \frac{1}{2} \frac{2f - 1}{3f - 2}. \tag{26}$$

Note that by putting $f = 1$ in above relation, one restores the size ratio of the ring and open linear chain of the same molecular weight (3). The quantity (26) decreases with the increasing branching parameter f and in the limit $f \rightarrow \infty$ reaches the asymptotic value $1/3$ (see figure 3).

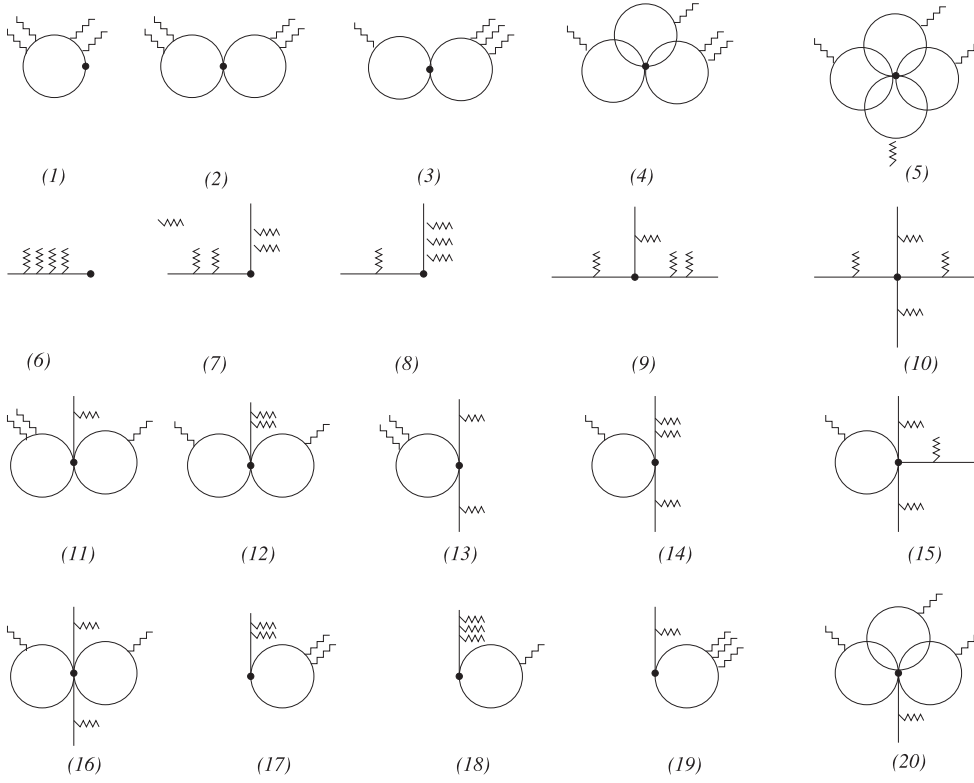


Figure 4. Diagrammatic presentation of contributions into $\langle \zeta(\vec{k}_1, \vec{k}_2) \rangle$. The wavy lines denote restriction points s_1, s_2, s_3, s_4 . With \bullet we denote the position of the starting branching point.

3.2. Asphericity

The products of the components of the gyration tensor (13) which appear in (16) can be calculated using the identity

$$\begin{aligned}
 & (\vec{r}_i^\alpha(s_2) - \vec{r}_j^\alpha(s_1)) (\vec{r}_i^\beta(s_2) - \vec{r}_j^\beta(s_1)) (\vec{r}_l^\alpha(s_4) - \vec{r}_m^\alpha(s_3)) (\vec{r}_l^\beta(s_4) - \vec{r}_m^\beta(s_3)) \\
 &= \frac{d}{dk_1^\alpha} \frac{d}{dk_1^\beta} \frac{d}{dk_2^\alpha} \frac{d}{dk_2^\beta} \zeta(\vec{k}_1, \vec{k}_2) \Big|_{\vec{k}_1=\vec{k}_2=0}
 \end{aligned} \tag{27}$$

with

$$\zeta(\vec{k}_1, \vec{k}_2) = e^{-\vec{k}_1(\vec{r}_i(s_2) - \vec{r}_j(s_1))} e^{-\vec{k}_2(\vec{r}_l(s_4) - \vec{r}_m(s_3))}. \tag{28}$$

Again, we will use the diagrammatic presentation of contributions into $\langle \zeta(\vec{k}_1, \vec{k}_2) \rangle$ (see figure 4). Applying the same rules of diagram calculation, as introduced in the previous subsection and evaluating the corresponding expressions, we find

$$\begin{aligned}
\langle Q_{\alpha\beta} Q_{\alpha\beta} \rangle = & f_1 D_{\alpha\beta|\alpha\beta}^{(1)} + \frac{f_1(f_1 - 1)}{2} (D_{\alpha\beta|\alpha\beta}^{(2)} + D_{\alpha\beta|\alpha\beta}^{(3)}) \\
& + \frac{f_1(f_1 - 1)(f_1 - 2)}{6} D_{\alpha\beta|\alpha\beta}^{(4)} + \frac{f_1(f_1 - 1)(f_1 - 2)(f_1 - 3)}{24} D_{\alpha\beta|\alpha\beta}^{(5)} \\
& + f_2 D_{\alpha\beta|\alpha\beta}^{(6)} + \frac{f_2(f_2 - 1)}{2} (D_{\alpha\beta|\alpha\beta}^{(7)} + D_{\alpha\beta|\alpha\beta}^{(8)}) \\
& + \frac{f_2(f_2 - 1)(f_2 - 2)}{6} D_{\alpha\beta|\alpha\beta}^{(9)} + \frac{f_2(f_2 - 1)(f_2 - 2)(f_2 - 3)}{24} D_{\alpha\beta|\alpha\beta}^{(10)} \\
& + \frac{f_1(f_1 - 1)f_2}{2} (D_{\alpha\beta|\alpha\beta}^{(11)} + D_{\alpha\beta|\alpha\beta}^{(12)}) \\
& + \frac{f_1 f_2 (f_2 - 1)}{2} (D_{\alpha\beta|\alpha\beta}^{(13)} + D_{\alpha\beta|\alpha\beta}^{(14)}) \\
& + \frac{f_1 f_2 (f_2 - 1)(f_2 - 2)}{6} D_{\alpha\beta|\alpha\beta}^{(15)} + \frac{f_1(f_1 - 1)f_2(f_2 - 2)}{4} D_{\alpha\beta|\alpha\beta}^{(16)} \\
& + f_1 f_2 (D_{\alpha\beta|\alpha\beta}^{(17)} + D_{\alpha\beta|\alpha\beta}^{(18)} + D_{\alpha\beta|\alpha\beta}^{(19)}) + \frac{f_1(f_1 - 1)(f_1 - 2)f_2}{6} D_{\alpha\beta|\alpha\beta}^{(20)}. \quad (29)
\end{aligned}$$

Here, $D_{\alpha\beta|\alpha\beta}^{(n)}$ denotes contribution of n th diagram on figure 4 (see appendix for details).

The resulting expression for the asphericity thus reads

$$\begin{aligned}
\hat{A}_{f_1 f_2} = & (2 + d) \left[8f_2^2 (15f_2 - 14) + f_1^2 (8f_1 - 7) \right. \\
& + 4f_1 f_2 (62f_1 + 28f_2 - 41) \left. \right] \times \left[5d \left(4f_2^2 (3f_2 - 2)^2 + f_1^2 (2f_1 + 1)^2 \right) \right. \\
& + 4f_1 f_2 \left(f_2^2 (72f_2 - 238) - f_1^2 (24f_1 + 113) + 196 \right) + 2f_1^2 (8f_1 - 7) \\
& \left. + 16f_2^2 (15f_2 - 14) + 8f_1 f_2 (62f_1 + 34f_2 - 41) \right]^{-1}. \quad (30)
\end{aligned}$$

The case $f_2 = 0$ corresponds to the rosette structure (figure 1(a)) with

$$\hat{A}_{\text{rosette}} = \frac{(2 + d)(8f_1 - 7)}{5d(2f_1 - 1)^2 + 2(8f_1 - 7)}, \quad (31)$$

at $f_1 = 1$, one restores the expression of the asphericity of an individual ring polymer (6). Note that, for the system of two bonded rings ($f_2 = 2$), we restore expression (6) in accordance with the numerical results of [48]. The case $f_1 = 0$ corresponds to star structure (figure 1(c)) with

$$\hat{A}_{\text{star}} = 2 \frac{(2 + d)(15f_2 - 14)}{5d(3f_2 - 2)^2 + 4(15f_2 - 14)}. \quad (32)$$

Again, at $f_2 = 1, 2$ one restores an expression of asphericity of an individual linear polymer (5).

To compare the degree of asphericity of rosette and star polymer structures of the same molecular weight (at $f_1 = f_2 = f$), we plot the above given quantities as functions of f at fixed $d = 3$ (see figure 5(a)). At small f , the star polymers are more anisotropic and extended in space than rosette structures, whereas both \hat{A}_{star} and \hat{A}_{rosette} gradually tend to zero with

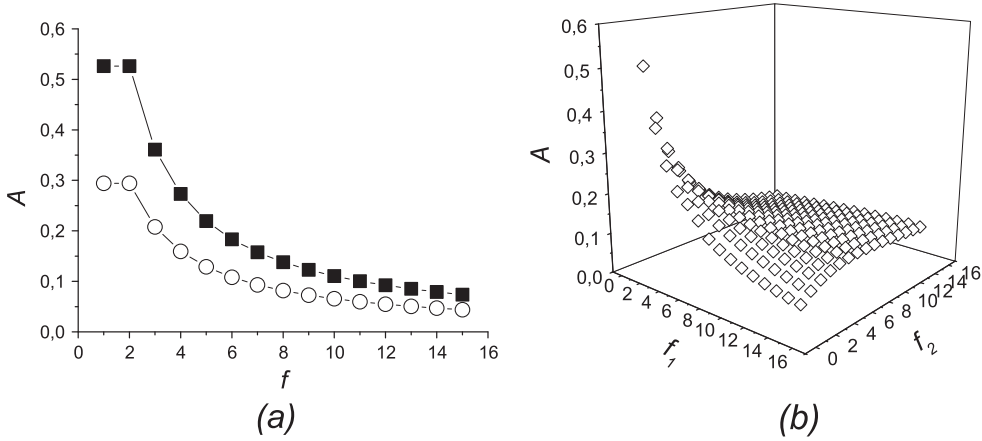


Figure 5. (a): Asphericity of rosette structure (31) (open circles) and star-like structure (32) (filled squares) of the same total molecular weight as functions of branching parameter f in space dimension $d = 3$. Lines are guides to the eyes. (b): Asphericity of the system consisting of f_1 polymer loops and f_2 linear branches (30) as function of f_1, f_2 in space dimension $d = 3$.

increasing f . Really, in the asymptotic limit $f \rightarrow \infty$ both the rosette and star structures can be treated as soft colloidal particles with highly symmetrical shape. The total asphericity of the system consisting of f_1 closed polymer loops and f_2 linear branches (equation (30)) is plotted as a function of f_1, f_2 at fixed $d = 3$ in figure 5(b). The value of this quantity is the result of the competition between two effects: decreasing asymmetry with an increasing number of closed loops and increasing degree of anisotropy with an increasing number of linear branches.

4. Conclusions

In this paper, we analysed the conformational properties of polymer systems of complex topologies (see figure 1). While the properties of so-called star polymers (figure 1(c)) have been intensively studied, much less is known about the details of rosette (figure 1(a)) and ring-linear (figure 1(b)) structures. Multiple loop formation in polymer macromolecules plays an important role in various biochemical processes such as DNA compactification [8–10], which makes the rosette-like structures interesting objects to study. Note that another possible interpretation of the structures (figures 1 (a) and (b)) is the following: they can be treated as projections of long flexible bulk polymer onto the two-dimensional plane [42].

Restricting ourselves to the idealized Gaussian case, when any interactions between monomers are neglected, we develop the continuous chain representation of the complex polymer model considering each of the individual branches or petals as a path of length S_i , parameterized by $\vec{r}_i(s)$, where s is varying from 0 to S_i ($i = 1, 2, \dots, f_1 + f_2$). The size and shape characteristics of a typical polymer conformation have been studied on the basis of the gyration tensor \mathbf{Q} with the components given by (13). Working within the framework of the path integration method and making use of appropriate diagram technique, we obtained the expressions for the gyration radius $\langle R_{g,f_1,f_2}^2 \rangle$ and asphericity \hat{A} , measuring the extent of anisotropy of a typical conformation of complex polymer structures, as functions of parameters f_1, f_2 . In particular, our analytical results quantitatively confirm the compactification

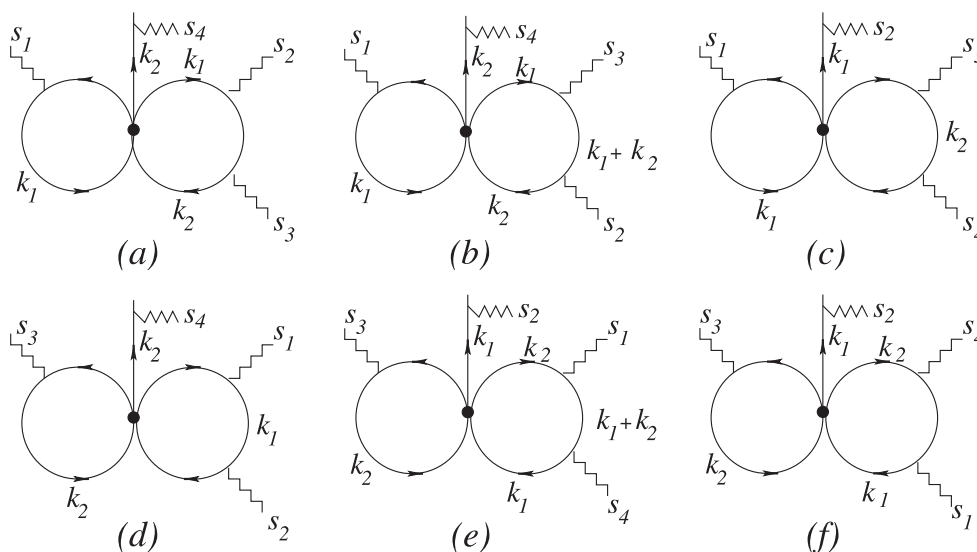


Figure 6. Diagram (11) on figure 4 with various permutations of restriction points s_1, s_2, s_3, s_4 .

(decrease of the effective size) of multiple loop polymer structures as compared with structures containing linear segments (equation (26)). A decrease of the anisotropy of rosette polymers as compared with star-like structures of the same total molecular weight is revealed as well (equations (31) and (32)).

Acknowledgments

This work was supported by the FP7 EU IRSES projects N269139 ‘Dynamics and Cooperative Phenomena in Complex Physical and Biological Media’ and N295302 ‘Statistical Physics in Diverse Realizations’. Financial support from the Academy of Finland within the FiDiPro scheme is acknowledged.

Appendix

Here, we evaluate the analytical expressions corresponding to diagram (11) on figure 4. Note that, in the diagram calculations, one should take into account the possible permutations of positions of restriction points s_1, s_2, s_3, s_4 (see figure 6).

The resulting expressions read:

$$\begin{aligned}
\zeta^{(11)a}(\vec{k}_1, \vec{k}_2) &= e^{-\frac{k_1^2}{2}(S-s_1+s_2)} e^{-\frac{k_2^2}{2}(S-s_3+s_4)} \int dq_1 \int dq_2 e^{-\frac{q_1^2}{2}S} e^{-\frac{q_2^2}{2}S} \\
&\quad \times e^{-q_1 k_1(S-s_1)} e^{-q_2 k_1 s_2} e^{-q_2 k_2(S-s_3)} \\
&= e^{-\frac{k_1^2}{2S}(S(s_1+s_2)-s_1^2-s_2^2)} e^{-\frac{k_2^2}{2S}(S(s_3+s_4)-s_3^2)} + \frac{k_1 k_2}{S} s_2(S-s_3), \\
\zeta^{(11)b} &= e^{-\frac{k_1^2}{2}(S-s_1+s_2)} e^{-\frac{k_2^2}{2}(S-s_3+s_4)} e^{-k_1 k_2(s_2-s_3)} \int dq_1 \int dq_2 e^{-\frac{q_1^2}{2}S} e^{-\frac{q_2^2}{2}S} \\
&\quad \times e^{-q_1 k_1(S-s_1)} e^{-q_2 k_1 s_2} e^{-q_2 k_2(S-s_3)} \\
&= e^{-\frac{k_1^2}{2S}(S(s_1+s_2)-s_1^2-s_2^2)} e^{-\frac{k_2^2}{2S}(S(s_3+s_4)-s_3^2)} + \frac{k_1 k_2}{S} (s_2(S-s_3) - S(s_2-s_3)), \\
\zeta^{(11)c} &= e^{-\frac{k_1^2}{2}(S-s_1+s_2)} e^{-\frac{k_2^2}{2}(s_4-s_3)} \int dq_1 \int dq_2 e^{-\frac{q_1^2}{2}S} e^{-\frac{q_2^2}{2}S} e^{-q_1 k_1(S-s_1)} \\
&\quad \times e^{-q_2 k_2(s_4-s_3)} = e^{-\frac{k_1^2}{2}(s_1+s_2) - \frac{k_2^2}{2S}(s_4-s_3)(S-s_4+s_3)}, \\
\zeta^{(11)d} &= e^{-\frac{k_1^2}{2}(s_2-s_1)} e^{-\frac{k_2^2}{2}(S-s_3+s_4)} \int dq_1 \int dq_2 e^{-\frac{q_1^2}{2}S} e^{-\frac{q_2^2}{2}S} e^{-q_1 k_2(S-s_3)} \\
&\quad \times e^{-q_2 k_1(s_2-s_1)} = e^{-\frac{k_1^2}{2S}(s_2-s_1)(S-s_2+s_1) - \frac{k_2^2}{2}(s_3+s_4)}, \\
\zeta^{(11)e} &= e^{-\frac{k_1^2}{2}(S-s_1+s_2)} e^{-\frac{k_2^2}{2}(S-s_3+s_4)} e^{-k_1 k_2(s_4-s_1)} \int dq_1 \int dq_2 e^{-\frac{q_1^2}{2}S} e^{-\frac{q_2^2}{2}S} \\
&\quad \times e^{-q_1 k_2(S-s_3)} e^{-q_2 k_1(S-s_1)} e^{-q_2 k_2 s_4} \\
&= e^{-\frac{k_1^2}{2S}(S(s_1+s_2)-s_1^2) - \frac{k_2^2}{2S}(S(s_3+s_4)-s_3^2-s_4^2) + \frac{k_1 k_2}{S}(s_4(S-s_1) - S(s_4-s_1))}, \\
\zeta^{(11)f} &= e^{-\frac{k_1^2}{2}(S-s_1+s_2)} e^{-\frac{k_2^2}{2}(S-s_3+s_4)} \int dq_1 \int dq_2 e^{-\frac{q_1^2}{2}S} e^{-\frac{q_2^2}{2}S} e^{-q_1 k_2(S-s_3)} \\
&\quad \times e^{-q_2 k_2 s_4} e^{-q_2 k_1(S-s_1)} \\
&= e^{-\frac{k_1^2}{2S}(S(s_1+s_2)-s_1^2) - \frac{k_2^2}{2S}(S(s_3+s_4)-s_4^2) + \frac{k_1 k_2}{S} s_4(S-s_1)}.
\end{aligned}$$

Taking derivatives over the components of k_1, k_2 in expressions above according to (27) and integrating over s_1, \dots, s_4 , one finally obtains the contributions $D_{\alpha\beta}^{(11)}$ in (29):

$$D_{\alpha\alpha}^{(11)} = \frac{59}{45} S^6, \quad D_{\alpha\alpha|\beta\beta}^{(11)} = \frac{11}{9} S^6, \quad D_{\alpha\beta|\alpha\beta}^{(11)} = \frac{2}{45} S^6. \quad (33)$$

References

- [1] Perry L J and Wetzel R 1984 *Science* **226** 555
- [2] Wells J A and Powers D B 1986 *J. Biol. Chem.* **261** 6564
- [3] Pace C N, Grimsley G R, Thomson J A and Barnett B J 1988 *J. Biol. Chem.* **263** 11820
- [4] Nagi A D and Regan L 1997 *Folding Des.* **2** 67
- [5] Schlieff R 1988 *Science* **240** 127
- [6] Rippe K, von Hippel P H and Langowski J 1995 *Trends Biochem. Sci.* **20** 500
- [7] Towles K B, Beausang J F, Garcia H G, Phillips R and Nelson P C 2009 *Phys. Biol.* **6** 025001
- [8] Fraser P 2006 *Curr. Opin. Genetics Dev.* **16** 490
- [9] Simonis M, Klous P, Splinter E, Moshkin Y, Willemsen R, de Wit E, van Steensel B and de Laat W 2006 *Nat. Genetics* **38** 1348
- [10] Dorier J and Stasiak A 2009 *Nucl. Acids Res.* **37** 6316
- [11] de Nooijer S, Wellink J, Mulder B and Bisseling T 2009 *Nucl. Acids Res.* **37** 3558

- [12] Chan H S and Dill K A 1989 *J. Chem. Phys.* **90** 492
- [13] Rey A and Freire J J 1991 *Macromolecules* **24** 4673
- [14] Rubio A M, Freire J J, Bishop M and Clarke J H R 1993 *Macromolecules* **26** 4018
- [15] Wittkop M, Kreitmeier S and Göritz D 1996 *J. Chem. Phys.* **104** 351
- [16] Zhou H-X 2001 *J. Phys. Chem.* **104** 6763
- [17] Cui T, Ding J and Chen J Z Y 2006 *Macromolecules* **39** 5540
- [18] Toan N N, Marenduzzo D, Cook P R and Micheletti C 2006 *Phys. Rev. Lett.* **97** 178302
- [19] Shin J, Cherstvy A G and Metzler R 2015 *Soft Matter* **11** 472
- [20] Bishop M and Saltiel C 1986 *J. Chem. Phys.* **85** 6728
- [21] Diehl H W and Eisenriegler E 1989 *J. Phys. A: Math. Gen.* **22** L87
- [22] Jagodzinski O, Eisenriegler E and Kremer K 1992 *J. Phys. I France* **2** 2243
- [23] Obukhov S P, Rubinstein M and Duke T 1994 *Phys. Rev. Lett.* **73** 1263
- [24] Muller M, Wittmer J P and Cates M E 2000 *Phys. Rev. E* **61** 4078
- [25] Deutsch J M 1999 *Phys. Rev. E* **59** R2539
- [26] Shimamura M K and Doguchi T 2001 *Phys. Rev. E* **64** 020801
- [27] Alim K and Frey E 2007 *Phys. Rev. Lett.* **99** 198102
- [28] Bohr M and Heermann D W 2010 *J. Chem. Phys.* **132** 044904
- [29] Calabrese P, Pelissetto A and Vicari E 2002 *J. Chem. Phys.* **116** 8191
- [30] Sakaue T 2011 *Phys. Rev. Lett.* **106** 167802
- [31] Jung Y, Jeon C, Kim J, Jeong H, Jun S and Ha B-Y 2012 *Soft Matter* **8** 2095
- [32] Rosa A, Orlandini E, Tubiana L and Micheletti C 2011 *Macromolecules* **44** 8668
- [33] Shin J, Cherstvy A G and Metzler R 2014 *New J. Phys.* **16** 053047
- [34] Cluzel P, Lebrun A, Heller C, Lavery R, Viovy J-L, Chatenay D and Caron F 1996 *Science* **271** 792
- [35] Yamaguchi H, Kubota K and Harada A 2000 *Nucleic Acids Symp. Ser.* **44** 229
- [36] Lyubchenko Y L, Shlyakhtenko L S, Binus M, Gaillard C and Strauss F 2002 *Nucleic Acids Res.* **30** 4902
- [37] Wang J C 1985 *Annu. Rev. Biochem.* **54** 665
- [38] Champoux J J 2001 *Annu. Rev. Biochem.* **70** 369
- [39] Krasnow M A and Cozzarelli N R 1982 *J. Biol. Chem.* **257** 2681
- [40] Duda R L 1998 *Cell* **94** 55
- [41] Zhou H-X 2003 *J. Am. Chem. Soc.* **125** 9280
- [42] Metzler R, Hanke A, Dommersnes P G, Kantor Y and Kardar M 2002 *Phys. Rev. Lett.* **88** 188101
- [43] Metzler R, Kantor Y and Kardar M 2002 *Phys. Rev. E* **66** 022102
- [44] Ercolini E, Valle F, Adamcik J, Metzler R, de los Rios P, Roca J and Dietler G 2007 *Phys. Rev. Lett.* **98** 058102
- [45] Wikoff W R, Liljas L, Duda R L, Tsuruta H, Hendrix R W and Johnson J E 2000 *Science* **289** 2129
- [46] Blankenship J W and Dawson P E 2003 *J. Mol. Biol.* **327** 537
- [47] Bohn M and Heermann D W 2010 *J. Chem. Phys.* **132** 044904
- [48] Bohn M, Heermann D W, Lourenc O and Cordeiro C 2010 *Macromolecules* **43** 2564
- [49] Duplantier B 1989 *J. Stat. Phys.* **54** 581
- [50] Schäfer L, von Ferber C, Lehr U and Duplantier B 1992 *Nucl. Phys. B* **374** 473
- [51] Grest G S, Kremer K and Witten T A 1987 *Macromolecules* **20** 1376
- [52] Hsu H P, Nadler W and Grassberger P 2004 *Macromolecules* **37** 4658
- [53] Ohno K and Binder K 1991 *J. Chem. Phys.* **95** 5444
- [54] Shida K, Ohno K, Kimura M and Kawazoe Y 1996 *J. Chem. Phys.* **105** 8929
- [55] von Ferber C and Holovatch Y 1995 *Condens. Matter Phys.* **5** 8
- [56] von Ferber C and Holovatch Y 1996 *Theor. Math. Phys.* **109** 1274
- [57] von Ferber C and Holovatch Y 2002 *Phys. Rev. E* **65** 042801
- [58] de Gennes P G 1979 *Scaling Concepts in Polymer Physics* (Ithaca: Cornell University Press)
- [59] des Cloizeaux J and Jannink G 1990 *Polymers in Solutions: Their Modelling and Structure* (Oxford: Clarendon)
- [60] Zimm H and Stockmayer W H 1949 *J. Chem. Phys.* **17** 1301
- [61] Prentis J J 1982 *J. Chem. Phys.* **76** 1574
- Prentis J J 1984 *J. Phys. A: Math. Gen.* **17** 1723
- [62] Baumgärtner A 1982 *J. Chem. Phys.* **76** 4275

- [63] Miyake A and Freed K F 1983 *Macromolecules* **16** 1228
Miyake A and Freed K F 1984 *Macromolecules* **17** 678
- [64] Alessandrini J L and Carignano M A 1992 *Macromolecules* **25** 1157
- [65] Bishop M M, Clarke J H R and Freire J J 1993 *J. Chem. Phys.* **98** 3452
- [66] Wei G 1997 *Macromolecules* **30** 2125
- [67] Dima R I and Thirumalai D 2004 *J. Phys. Chem. B* **108** 6564
Hyeon C, Dima R I and Thirumalai D 2006 *J. Chem. Phys.* **125** 194905
- [68] Rawat N and Biswas P 2009 *J. Chem. Phys.* **131** 165104
- [69] Hu T, Grosberg A Y and Shklovskii B I 2006 *Biophys. J.* **90** 2731
- [70] Kuhn W 1934 *Kolloid-Z* **68** 2
Herzog R O, Illig R and Kudar H 1934 *Z. Physik. Chem. Abt. A* **167** 329
Perrin F 1936 *J. Phys. Radium* **7** 1
- [71] Aronovitz J A and Nelson D R 1986 *J. Physique* **47** 1445
- [72] Rudnick J and Gaspari G 1986 *J. Phys. A: Math. Gen.* **19** L191
Gaspari G, Rudnick J and Beldjenna A 1987 *J. Phys. A: Math. Gen.* **20** 3393
- [73] Wei G and Eichinger B E 1996 *J. Chem. Phys.* **104** 9142
- [74] Behamou M and Mahoux G 1985 *J. Phys. Lett.* **46** L689
- [75] Domb C and Hioe F T 1969 *J. Chem. Phys.* **51** 1915
- [76] Bishop M and Saltiel C J 1988 *J. Chem. Phys.* **88** 6594
- [77] Honeycutt J D and Thirumalai D 1988 *J. Chem. Phys.* **90** 4542
- [78] Drube F, Alim K, Witz G, Dietler G and Frey E 2010 *Nano Lett.* **10** 1445
- [79] Solc K and Stockmayer W H 1971 *J. Chem. Phys.* **54** 2756
Solc K 1971 *J. Chem. Phys.* **55** 335
- [80] Edwards S F 1965 *Proc. Phys. Soc. London* **85** 613
Edwards S F 1965 *Proc. Phys. Soc. London* **88** 265